

Received July 21, 2019, accepted September 11, 2019, date of publication September 13, 2019, date of current version October 24, 2019.

Digital Object Identifier 10.1109/ACCESS.2019.2941364

Disturbance-Observer-Based Sliding Mode Control Design for Nonlinear Unmanned Surface Vessel With Uncertainties

ZHENG CHEN^{1,2}, (Senior Member, IEEE), YOUGONG ZHANG², YOUMING ZHANG²,
YONG NIE¹, JIANZHONG TANG¹, AND SHIQIANG ZHU^{2,3}

¹State Key Laboratory of Fluid Power and Mechatronic Systems, Zhejiang University, Hangzhou 310027, China

²Ocean College, Zhejiang University, Zhoushan 316021, China

³Zhejiang Lab, Hangzhou 311100, China

Corresponding author: Yong Nie (ynie@zju.edu.cn)

This work was supported in part by the Natural Science Foundation of Zhejiang Province, China, under Grant LY19E050016, in part by the National Natural Science Foundation of China under Grant 61603332, and in part by the Fundamental Research Funds for the Central Universities.

ABSTRACT Unmanned surface vessel (USV) has been widely applied due to its advantages in the maritime security inspection and resources exploration. Good trajectory tracking performance is a critical issue in the control design of USV. However, most of the existing controllers are designed based on linear dynamic model or do not well consider the integrated effect nonlinearities, various uncertainties (e.g., modeling error and parameter variations) and external disturbance (wind, wave, current, etc). In this paper, a nonlinear dynamic model is established for USV with the integrate consideration of these issues, and a disturbance-observer-based sliding mode control design is subsequently proposed to achieve the good tracking performance, where the observer is to estimate and compensate the modeling uncertainties and external disturbance. Theoretically, the stability of the observer and overall closed-loop system of USV are guaranteed via the Lyapunov theorem. The comparative simulation is carried out, and the results show the fast response, better transient performance and robustness of the proposed control design.

INDEX TERMS Sliding mode control, disturbance observer, unmanned surface vessel (USV), Lyapunov stability theorem.

I. INTRODUCTION

The maritime security inspection and resources exploration have raised much attention in recent years. As an transport platform, unmanned surface vessel (USV) can undertake the long-time, wide-range and low-cost oceanic tasks. With the development of advanced mechatronics [1]–[4], the USV has been applied in a wide range of military and commercial application fields [5]–[8], such as environmental inspection, geophysical exploration, oceanic data collection, maritime search and rescue, etc.

With the complex working conditions include wind, wave and current, the nonlinear USV has become a hotspot, and to achieve the precise trajectory tracking is still challenging [9], [10]. The linearization of nonlinear dynamics for USV and the corresponding linear control design is an effective

approach, which will have good performance around the specific equilibrium point. Namely, Jongho Shin *et al.* [11] proposes an adaptive path-following control algorithm for an USV based on an identified linear dynamic model, where the virtual control input, dynamic surface and adaptive terms are used to deal with matched and unmatched uncertainties. Ning Wang *et al.* [12] proposed a finite-time observer based control scheme for the USV tracking with time-varying and large slideslip angles and unknown external disturbances. Subsequently, a fuzzy unknown observer is designed in [13] to estimate multiple unknowns of USV including unmodeled dynamics, uncertainties and disturbances. Though these studies with linear USV model have good capacity of path tracking at specific equilibrium point, they are only suitable for some specific trajectories (e.g., straight-line path). Actually, the USV is not always working at the specific equilibrium point, and there exists the external disturbance from the complex oceanic conditions (wind, wave, current, etc),

The associate editor coordinating the review of this manuscript and approving it for publication was Jinpeng Yu.

which can result in the USV away from the equilibrium point, and even exacerbate the USV's tracking performances [14]. Besides, the various uncertainties (e.g., modeling error and parameter variations) in the USV cannot be well handled with the aforementioned linear USV model. Thus, the approach to linearize USV dynamic model cannot be well applied in the consideration of nonlinearities, various uncertainties and external disturbance.

Recently, in view of the above issues, some relevant nonlinear control algorithms have been conducted [15]–[19], such as back-stepping control, sliding mode control, model predictive control, network-based control, etc. Jianda Han *et al.* [20] developed a nonlinear modeling scheme—the active modeling enhanced quasi-linear parameter-varying model for a water-jet propulsion USV system. A nonlinear version of the Kalman filter-based active modeling method is developed to estimate the unstructured model to eliminate the modeling errors. To improve the transient performance for path-following control of USV with oceanic disturbances, Chuan Hu *et al.* [21] proposed a disturbances observer-based composite nonlinear feedback controller, which could restrain system overshoots and eliminate steady-state errors while dealing with multiple oceanic disturbances. Lokukaluge P.Perera, *et al.* [22] proposed a pre-filter based sliding mode approach to control the USV steering system, which does not require accurate dynamics and could deal with bounded disturbances. Bong Seok Park, *et al.* [23] developed an adaptive output feedback controller for trajectory tracking of USV by simultaneously considering the input saturation and underactuated problems. Moreover, considering the realistic model of USV with uncertainties, an adaptive observer based on the neural networks is designed in [23] to estimate the velocity of USV. Considering input saturation and modeling uncertainties, an adaptive sliding model controller is proposed in [24] for an underactuated USV using neural network, auxiliary dynamic system, and backstepping technique. To solve the problem of trajectory tracking of an underactuated surface vessel, Zhijian Sun, *et al.* [25] designed a PI sliding mode controller with a continuous adaptive term which is constructed to reduce the chattering problem. To achieve accurate trajectory tracking of USV with complex marine environments, a finite-time nonsingular fast terminal sliding control scheme are proposed by Wang *et al.* [26]. Specifically, the finite-time disturbance observer proposed in [27] and [28] is designed to estimate the unknown external disturbances from complex ocean winds, waves and currents.

Though several control algorithms are tried to achieve better tracking performance, few related works consider the integrated influence including the nonlinearities, various uncertainties and external disturbance. Thus, a nonlinear dynamic model considering various uncertainties (e.g., modeling error and parameter variations) and external disturbances (e.g., wind, wave, current) for USV is established in this paper. Subsequently, a disturbance-observer-based sliding mode control design is developed to achieve the good tracking performance, where the observer is designed

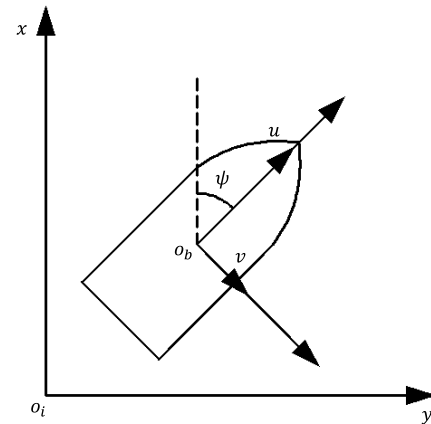


FIGURE 1. The model of USV.

to estimate and compensate the modeling uncertainties and external disturbance, and a saturation function is designed to avoid the chattering phenomenon of the traditional sliding mode control. Based on the Lyapunov stability theorem, the stability of the observer and overall closed-loop system of USV are guaranteed. The comparative simulations with different controllers and different desired trajectory are carried out and the results show the priority and effectiveness of proposed control design.

The remainder of this paper is organized as follows. Section 2 describes the nonlinear modeling and linear modeling of the USV system. Section 3 formulates the design of the slide-mode controller, the design and stability analysis of disturbance observer, and the stability analysis of overall closed-loop system. Section 4 presents the comparative trajectory tracking simulation with different controllers and its analysis. Finally, Section 5 describes the contributions of this paper and future research.

II. USV SYSTEM MODELING

A. NONLINEAR MODELING

The USV model can be described as a 3-DOF system. Through constructing ground coordination and body coordination as in Fig.1. The kinematic model of the USV in the planar motion can be described as follows:

$$\dot{\eta} = R(\psi) V \quad (1)$$

where, $\eta = [x \ y \ \psi]^T$, $V = [u \ v \ r]^T$,

$$R(\psi) = \begin{bmatrix} \cos \psi & -\sin \psi & 0 \\ \sin \psi & \cos \psi & 0 \\ 0 & 0 & 1 \end{bmatrix} \quad (2)$$

where x , y and ψ are the global coordination of the USV, u , v and r are the translational velocities and yaw rotational velocity, respectively, as shown in Fig.1, $R(\psi)$ is the rotation matrix form frame $\{b\}$ to frame $\{i\}$.

The nonlinear dynamic model of the USV can be described as:

$$M\dot{V} + CV + DV = \tau + d \quad (3)$$

where $\tau \left(\begin{bmatrix} \tau_x & \tau_y & \tau_n \end{bmatrix}^T \right)$ is the control vector. M is the inertial matrix, C is the matrix of Coriolis, and centripetal term. D is damping matrix, d represents the uncertain dynamics (model uncertainty and the external disturbances). The matrices M, C and D can be described as follows. In this paper, we assume that η and V are measurable.

$$M = \begin{bmatrix} m - X_{\dot{u}} & 0 & 0 \\ 0 & m - Y_{\dot{v}} & mx_G - Y_{\dot{r}} \\ 0 & mx_G - N_{\dot{v}} & I_{zz} - N_{\dot{r}} \end{bmatrix} \quad (4)$$

where m is the USV's mass. I_{zz} is the USV's moment of inertia about the rotational vertical axis passing through the origin of the body coordination. x_G is the position of the gravity center. X_* , Y_* , Z_* are hydrodynamic coefficients.

$$C = \begin{bmatrix} 0 & 0 & -m_{22}v - m_{23}r \\ 0 & 0 & m_{11}u \\ m_{22}v + m_{23}r & -m_{11}u & 0 \end{bmatrix} \quad (5)$$

and

$$D = - \begin{bmatrix} X_u & 0 & 0 \\ 0 & Y_v & Y_r \\ 0 & N_v & N_r \end{bmatrix} \quad (6)$$

where m_{ij} is the element of inertial matrix M .

For the water-jet USV, the water-jet propulsion produces the driving forces and torque, which follow these equations:

$$\tau = \begin{bmatrix} \tau_x \\ \tau_y \\ \tau_n \end{bmatrix} = \begin{bmatrix} T \cos \delta_r \\ -T \sin \delta_r \\ x_{\delta_r} T \sin \delta_r \end{bmatrix} \quad (7)$$

where T is the water-jet propulsion force, δ_r is the rudder angle, the x_{δ_r} is the distance from the water-jet nozzle to the gravity center o_b (shown in Fig.1).

Property 1 : $\dot{M} - 2C$ is skew-symmetric.

Assumption 1 : The external disturbances d is bounded by $d \leq d^*$, where d^* is unknown positive constants. Simultaneously, due to that the disturbances d are usually considered to be superimposed by the low frequency period signals in the most working conditions [12], thus it is assumed to have a low change rate, which mean $\dot{d} = 0$.

B. LINEAR MODELING

To better analyze the performance of proposed control design near the equilibrium point, the USV is modeled near the equilibrium point in this section, the detailed analysis is in the following.

Define the equilibrium point as [11]:

$$u = u_0, \quad v = 0, \quad r = 0, \quad \delta_r = 0, \quad T = T_0 \quad (8)$$

Then, the surge dynamics can be derived with (3) and (8):

$$\Delta \dot{u} = a_u \Delta u + b_u \Delta T \quad (9)$$

where $\Delta u = u - u_0$, $\Delta T = T - T_0$, $a_u = \frac{X_u}{m - X_{\dot{u}}}$, $b_u = \frac{1}{m - X_{\dot{u}}}$.

With the Nomoto's steering model [11], the turn rate r is represented as a simple first-order dynamics with the rudder angle δ_r :

$$\tau_r \Delta \dot{r} + \Delta r = b_r \Delta \delta_r \quad (10)$$

where $b_r = \frac{T_0 x_{\delta_r}}{I_{zz} - N_{\dot{r}}}$.

Suppose u is almost unchanged and the yaw perturbation is small, the sway dynamics can be described as:

$$\tau_\beta \Delta \dot{\beta} + \Delta \beta = -K_\beta \Delta r \quad (11)$$

where β is the sideslip angle, $\Delta \beta = \text{atan2} \left(\frac{\Delta v}{\Delta u} \right)$ and atan2 is an inverse function of the tangent function defined between $-\pi$ and π .

According to the above derivation (9)-(11), the linearized USV model can be summarized as follows:

$$\dot{x} = Ax + B\delta + \Delta \quad (12)$$

where $x = [u \ \beta \ \psi \ r]^T$, $\delta = [T \ \delta_r]^T$,

$$A = \begin{bmatrix} a_u & 0 & 0 & 0 \\ 0 & -\frac{1}{\tau_\beta} & 0 & -\frac{K_\beta}{\tau_\beta} \\ 0 & 0 & 0 & 1 \\ 0 & 0 & 0 & -\frac{1}{\tau_r} \end{bmatrix} \quad (13)$$

$$B = \begin{bmatrix} b_u & 0 \\ 0 & 0 \\ 0 & 0 \\ 0 & \frac{b_r}{\tau_r} \end{bmatrix} \quad (14)$$

The control objective is to design a dynamic output feedback controller with nonlinear dynamic model (3) or linear dynamic model (12). With these controllers, the USV can track the desired trajectory: $\eta_d = [x_d \ y_d \ \psi_d]^T$, $\dot{\eta}_d = [\dot{x}_d \ \dot{y}_d \ \dot{\psi}_d]^T$, $\ddot{\eta}_d = [\ddot{x}_d \ \ddot{y}_d \ \ddot{\psi}_d]^T$, where the η_d , $\dot{\eta}_d$, $\ddot{\eta}_d$ are continuous and bounded.

III. THE SLIDING MODE CONTROL DESIGN WITH DISTURBANCE-OBSERVER

In this section, based on the reference trajectory η_d , $\dot{\eta}_d$, $\ddot{\eta}_d$ produced by the USV desired tracking planner, a disturbance-observer-based sliding mode controller is designed in Fig.2 using the nonlinear dynamic model of USV (3), where a disturbance-observer is designed to estimate and compensate the effect of various uncertainties (e.g., modeling error and parameter variations) and external disturbance (wind, wave, current, etc). Then, the overall stability of a closed-loop system is rigorously analyzed using the Lyapunov stability theorem.

A. CONTROLLER DESIGN

Define the sliding surface s [29]–[32] as:

$$s = Ke + \dot{e} \quad (15)$$

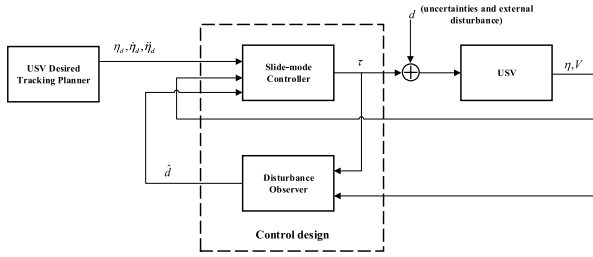


FIGURE 2. Disturbance-observer-based sliding mode control architecture for nonlinear USV system.

where $e = \eta - \eta_d$, $K = \text{diag}\{k_1, \dots, k_i, \dots, k_w\}$, $i = 1, 2, \dots, w$. Then the derivative of s can be calculated as:

$$\begin{aligned} \dot{s} &= K(\dot{\eta} - \dot{\eta}_d) + (\ddot{\eta} - \ddot{\eta}_d) \\ &= KR(\psi)V + \dot{R}(\psi)V + R(\psi)\dot{V} - K\dot{\eta}_d - \ddot{\eta}_d \\ &= KR(\psi)V + \dot{R}(\psi)V - K\dot{\eta}_d - \ddot{\eta}_d \\ &\quad + R(\psi)M^{-1}(\tau + d - (C + D)V) \end{aligned} \quad (16)$$

where $\dot{\eta} = \dot{R}(\psi)V + R(\psi)\dot{V}$, which can be derived according to kinematic model (1).

Therefore, the control law τ for the USV can be designed as [33]–[37]:

$$\begin{aligned} \tau &= MR(\psi)^{-1} \left(K\dot{\eta}_d + \ddot{\eta}_d - \dot{R}(\psi)V - \varepsilon M^{-1} \text{sat}(s) \right. \\ &\quad \left. - M^{-1}Cs \right) - (MK - C - D)V - \hat{d} \end{aligned} \quad (17)$$

where, \hat{d} is the nonlinear disturbance observer, which is designed in the next subsection, $\text{sat}(s)$ is a saturation function to avoid the chattering phenomenon, which is designed as:

$$\text{sat}(s) = \begin{cases} 1 & s > \Delta \\ \frac{1}{\Delta}s & \|s\| \leq \Delta \\ -1 & s < -\Delta, \end{cases} \quad (18)$$

Δ is the positive boundary layer.

B. DISTURBANCE-OBSERVER DESIGN

To observe the modeling uncertainties and external disturbance of the USV, the disturbance observer \hat{d} is designed as follows:

$$\begin{cases} \dot{\hat{d}} = L(CV + DV - \tau) - L\hat{d} \\ \hat{d} = Z + P \end{cases} \quad (19)$$

where,

$$L = H^{-1}M^{-1} \quad (20)$$

$$P = H^{-1}V \quad (21)$$

H is an invertible constant matrix, which can be calculated by the Linear Matrix Inequality (LMI). \hat{d} is the estimate value of the modeling uncertainties and external disturbance.

Since M and L are constants, the derivative of P can be calculated from (20) and (21):

$$\dot{P} = LM\dot{V} \quad (22)$$

As $\tilde{d} = d - \hat{d}$ is the observation error of disturbance d , the derivative of \tilde{d} can be calculated as:

$$\begin{aligned} \dot{\tilde{d}} &= \dot{d} - \dot{\hat{d}} = \dot{d} - \dot{Z} - \dot{P} \\ &= \dot{d} - L(CV + DV - \tau - P) + LZ - LM\dot{V} \\ &= \dot{d} + L(Z + P) - L(M\dot{V} + CV + DV - \tau) \\ &= \dot{d} + L\hat{d} - Ld \\ &= \dot{d} - L\tilde{d} \end{aligned} \quad (23)$$

With regard to Assumption 1, the observation error function can be derived as:

$$\dot{\tilde{d}} + L\tilde{d} = 0 \quad (24)$$

Then,

$$\dot{\tilde{d}} = -L\tilde{d} = -H^{-1}M^{-1}\tilde{d} \quad (25)$$

$$\dot{\tilde{d}}^T = -\tilde{d}^T M^{-T} H^{-T} \quad (26)$$

Define the Lyapunov Function V_d as:

$$V_d = \tilde{d}^T H^T M H \tilde{d} \quad (27)$$

where M is a positive definite matrix. Then the derivative of V_d can be calculated as:

$$\begin{aligned} \dot{V}_d &= \dot{\tilde{d}}^T H^T M H \tilde{d} + \tilde{d}^T H^T M H \dot{\tilde{d}} + \tilde{d}^T H^T \dot{M} H \tilde{d} \\ &= -\tilde{d}^T M^{-T} H^{-T} H^T M H \tilde{d} - \tilde{d}^T H^T M H H^{-1} M^{-1} \tilde{d} \\ &= -\tilde{d}^T H \tilde{d} - \tilde{d}^T H^T \tilde{d} \\ &= -\tilde{d}^T (H + H^T) \tilde{d} \end{aligned} \quad (28)$$

In order to satisfy $\dot{V}_d \leq -\tilde{d}^T \gamma \tilde{d}$, the following inequality is constructed as:

$$H + H^T \geq \gamma \quad (29)$$

where γ is a positive definite matrix.

The LMI approach is used to calculate the H satisfying (29), where the detailed calculation is in the following.

Define $Q = H^{-1}$, the (29) can be derived as:

$$Q^T + Q - Q^T \gamma Q \geq 0 \quad (30)$$

The Schur complement, which can be defined as: If C is the positive definite matrix, $A - BC^{-1}B^T \geq 0$ is equal to $\begin{bmatrix} A & B \\ B^T & C \end{bmatrix} \geq 0$, then (30) can be rewritten as:

$$\begin{bmatrix} Q^T + Q & Q^T \\ Q & \gamma^{-1} \end{bmatrix} \geq 0 \quad (31)$$

There exists Q satisfying the inequality (31), which can be calculated by the LMI toolbox in Matlab. As $H = Q^{-1}$, the desired H in (20) can be calculated to satisfy the inequality (29). Thus, $\dot{V}_d \leq -\tilde{d}^T \gamma \tilde{d} \leq 0$. As $V_d \geq 0$ and $\dot{V}_d \leq 0$, \tilde{d} is bounded, and $\dot{\tilde{d}} = 0$ when $V = 0$, which means the disturbance observer \hat{d} is asymptotically stable, and the observation error $\tilde{d} \rightarrow 0$ as $t \rightarrow \infty$.

C. OVERALL STABILITY ANALYSIS

Consider the closed-loop nonlinear USV system, one theorem to guarantee the closed-loop stability of the whole system can be obtained as:

Theorem : With the uncertainties and external disturbances, by applying the controller (17) with the nonlinear disturbance observer (19), the closed-loop nonlinear USV system is stable, and all the signals are bounded with the design of Lyapunov Function $V_m = V_s + V_d$. Furthermore, if $\|s\| \leq \Delta$, the Lyapunov Function V_m will be bounded by

$$V_m(t) \leq e^{-\sigma t} V_s(0) + \frac{\mu}{\sigma} (1 - e^{-\sigma t}) \quad (32)$$

Proof : Define the Lyapunov Function V_m for the closed-loop USV system as:

$$V_m = V_s + V_d \quad (33)$$

where $V_s = \frac{1}{2} s^T M s$, $V_d = \tilde{d}^T H^T M H \tilde{d}$.

The derivative of V_m can be calculated as:

$$\dot{V}_m = s^T M \dot{s} + \frac{1}{2} s^T \dot{M} s + \dot{V}_d \quad (34)$$

For

$$M \dot{s} = -\varepsilon \text{sat}(s) - C s + MR(\psi) M^{-1} \tilde{d} \quad (35)$$

Then

$$\dot{V}_m = s^T \left(-\varepsilon \text{sat}(s) - C s + MR(\psi) M^{-1} \tilde{d} \right) + \frac{1}{2} s^T \dot{M} s + \dot{V}_d \quad (36)$$

If $\|s\| > \Delta$, then the derivative of V_m can be calculated as:

$$\dot{V}_m = -\varepsilon \|s\| + s^T MR(\psi) M^{-1} \tilde{d} + \frac{1}{2} s^T (\dot{M} - 2C) s + \dot{V}_d \quad (37)$$

As the disturbance observer \dot{V}_d are asymptotically stable, $\|\tilde{d}\| \leq \|\tilde{d}(0)\|$. Let the norm of ε as:

$$\|\varepsilon\| > \left\| MR(\psi) M^{-1} \tilde{d}(0) \right\| \quad (38)$$

Then

$$\begin{aligned} \dot{V}_m &\leq -\left(\|\varepsilon\| - \left\| MR(\psi) M^{-1} \tilde{d}(0) \right\| \right) \|s\| + \dot{V}_d \\ &\leq -\left(\|\varepsilon\| - \left\| MR(\psi) M^{-1} \tilde{d}(0) \right\| \right) \|s\| - \tilde{d}^T \gamma \tilde{d} \end{aligned} \quad (39)$$

As $V_m \geq 0$ and $\dot{V}_m \leq 0$, s, \tilde{d} are bounded, and e, \dot{e} are bounded. Furthermore, $s = 0, \tilde{d} = 0$ when $\dot{V} = 0$, which means the closed-loop nonlinear USV system is asymptotically stable when $\|s\| > \beta$, and $e \rightarrow 0, \tilde{d} \rightarrow 0$ as $t \rightarrow \infty$.

If $\|s\| \leq \Delta$, then the derivative of V_m can be calculated as:

$$\begin{aligned} \dot{V}_m &= -\frac{\varepsilon}{\Delta} s^T s + s^T MR(\psi) M^{-1} \tilde{d} + \frac{1}{2} s^T (\dot{M} - 2C) s \\ &\quad - \tilde{d}^T \gamma \tilde{d} \\ &= -\sigma V_m + \mu \end{aligned} \quad (40)$$

TABLE 1. Principle parameters of USV [27], [38].

Parameter	Value	Parameter	Value
m	23.8	N_r	-1.9
I_{zz}	1.76	$X_{\dot{u}}$	-2.0
X_G	0.046	$Y_{\dot{v}}$	-10.0
X_u	-0.72253	$Y_{\dot{r}}$	-0.1
Y_v	-0.88965	$N_{\dot{v}}$	0
Y_r	-7.25	$N_{\dot{r}}$	-0.1
N_v	0.0313		

where $\mu = s^T MR(\psi) M^{-1} \tilde{d} - \tilde{d}^T \gamma \tilde{d}$ is quite small as $\tilde{d} \rightarrow 0$ when $t \rightarrow \infty$. It follows that

$$V_m(t) \leq e^{-\sigma t} V_s(0) + \frac{\mu}{\sigma} (1 - e^{-\sigma t}) \quad (41)$$

which leads to (32), and s, \tilde{d} are bounded. Then e, \dot{e} are bounded, and the control inputs τ are bounded. Thus, all the signals in nonlinear USV system are bounded when $\|s\| \leq \Delta$. The proof of *Theorem* is complete.

Based on the above proof, all the signals in the nonlinear USV system are bounded. With the design of nonlinear disturbance observer (19) in the controller (17), the modeling uncertainties and external disturbances d can be greatly observed, where the observation errors $\tilde{d} \rightarrow 0$ as $t \rightarrow 0$. With the design of the controller (17), $\eta \rightarrow \eta_d$, the good position tracking performance is achieved.

IV. SIMULATION

A. SIMULATION SETUP

To demonstrate the tracking performance of proposed control design, the comparative simulation is implemented on a benchmark prototype CyberShip II [27], [38], whereby principal parameters are summarized in Table 1:

To illustrate the performance of the proposed control design, three controllers are compared, as shown below:

C1: *Adaptive controller with linear identified USV model* (proposed in [11]). The control parameters are specified as $k_v = 100, k_{c1} = 1, k_{c2} = 1, d_w = 0.1, \tau = 0.1, \gamma_u = \gamma_\beta = \gamma_r = 0.01$.

C2: *PID controller with nonlinear USV model*. The control law is designed as:

$$\tau = R(\psi)^{-1} \left(K_p (\eta_d - \eta) + K_d (\dot{\eta}_d - \dot{\eta}) + K_i \int (\eta_d - \eta) dt \right) \quad (42)$$

where $K_p = \text{diag}\{100, 100, 100\}, K_d = \text{diag}\{100, 100, 100\}, K_i = \text{diag}\{20, 20, 20\}$.

C3: *Disturbance - observer - based sliding mode controller with nonlinear USV model*. The control law and disturbance observer are selected as (17) and (19), where $K = \text{diag}\{10, 10, 10\}, \varepsilon = \text{diag}\{100, 100, 100\}$ with regard to (38). In the disturbance observer (19), let $\gamma = \text{diag}\{0.1, 0.1, 0.1\}$, then H can be calculated by LMI toolbox with regard to (29), and the result is $H = \text{diag}\{0.1309, 0.1309, 0.1309\}$.

To testify the robustness of the proposed controller, the complex modeling uncertainties and external disturbances are assumed to be:

$$d = \begin{bmatrix} 15 + 0.2\sin\left(0.1\pi t - \frac{\pi}{3}\right) + 0.3\cos\left(0.3\pi t + \frac{\pi}{4}\right) \\ 17 + 0.3\sin\left(0.2\pi t + \frac{\pi}{4}\right) + 0.4\cos\left(0.1\pi t - \frac{\pi}{6}\right) \\ 19 + 0.5\sin\left(0.3\pi t + \frac{\pi}{6}\right) + 0.15\cos\left(0.2\pi t - \frac{\pi}{3}\right) \end{bmatrix} \quad (43)$$

In addition, to make comparisons on the proposed control design with other counterparts in terms of both transient response and steady-state tracking performance, MIAC index [39] is used to evaluate it, which is designed as:

$$MIAC = \frac{1}{t_f - t_0} \int_{t_0}^{t_f} |j_e| dt \quad (44)$$

where j_e represents the tracking errors x_e, y_e, ψ_e, t_0 and t_f represent the start time and end time of simulation.

To make the trajectory tracking performance persuasive, the desired trajectory consist of straight lines and circles, which can represent somewhat realistic tracking performance in practical engineering. Two simulation sets with different desired trajectory are designed as follows:

- SET1: Trajectory around the specific equilibrium point
- SET2: Trajectory apart from the specific equilibrium point

B. SIMULATION OF SET1

In order to evaluate the trajectory tracking performance around the specific equilibrium point, the desired trajectory is selected as (45)-(47) and Fig.3.

$$x_d = \begin{cases} 30 & t \leq T_1 \\ 18 + 12\cos(0.25(t - T_1)) & T_1 < t \leq T_2 \\ 18 - 12\sin(0.25(t - T_2)) & T_2 < t \leq T_3 \\ 6 & T_3 < t \leq T_4 \end{cases} \quad (45)$$

$$y_d = \begin{cases} 3t & t \leq T_1 \\ 30 + 12\sin(0.25(t - T_1)) & T_1 < t \leq T_2 \\ 54 - 12\cos(0.25(t - T_2)) & T_2 < t \leq T_3 \\ 54 + 3(t - T_3) & T_3 < t \leq T_4 \end{cases} \quad (46)$$

$$\psi_d = \begin{cases} \frac{\pi}{2} & t \leq T_1 \\ \frac{\pi}{2} + 0.25(t - T_1) & T_1 < t \leq T_2 \\ \pi - 0.25(t - T_2) & T_2 < t \leq T_3 \\ \frac{\pi}{2} & T_3 < t \leq T_4 \end{cases} \quad (47)$$

where $T_1=10, T_2=10+2\pi, T_3=10+4\pi, T_4=20+4\pi$. The initial condition of the USV in SET1 are set as: $x(0) = 30, y(0) = 0, \psi(0) = \frac{\pi}{2}, u(0) = 3, v(0) = 0, r(0) = 0$.

The comparative simulation results are shown in Fig.4-Fig.5. Fig.4(a) presents the trajectory tracking performance of USV with C1, C2 and C3 respectively. It can be observed that the USV follows the desired trajectory accurately and smoothly under complex uncertainties including external disturbances and unmodeled dynamics (43). In the meantime,

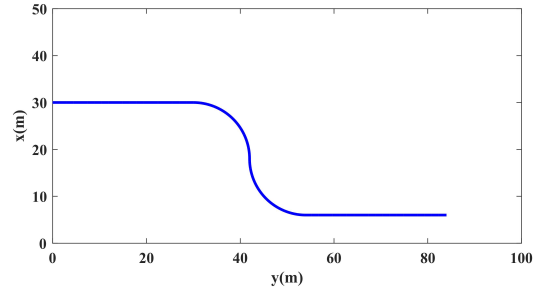


FIGURE 3. The desired trajectory of USV in SET1.

TABLE 2. MIAC of SET1 among different controllers.

MIAC	Value
C1:controller proposed in [11]	$MIAC_{x_e} = 0.0400$
	$MIAC_{y_e} = 0.1323$
	$MIAC_{\psi_e} = 0.0051$
C2:PID controller	$MIAC_{x_e} = 0.0270$
	$MIAC_{y_e} = 0.0180$
	$MIAC_{\psi_e} = 0.0251$
C3:proposed control design	$MIAC_{x_e} = 0.0066$
	$MIAC_{y_e} = 0.0096$
	$MIAC_{\psi_e} = 0.0029$

the corresponding tracking errors of all control algorithms are shown in Fig.4(b), which can effectively achieve ultimately bounded within a reasonable range, implying the stability and effectiveness of control design. Table 2 shows the MIAC value of different controllers in SET1. It can be seen that $MIAC_{x_e}$ of C3 is 16.50% of C1 and 24.44% of C2, $MIAC_{y_e}$ of C3 is 7.26% of C1 and 53.33% of C2, and $MIAC_{\psi_e}$ of C3 is 56.86% of C1 and 11.55% of C2, which reflects that the proposed control design has better transient response performance and robustness than linear controller and PID controller with the trajectory around the specific equilibrium point.

Moreover, the estimate performance of observer (19) is depicted in Fig.5(a), where the red curve represents the estimate value of disturbance and the blue curve represents the estimate value of observer (19). Simultaneously, the estimate error is showed in Fig.5(b), which can be closer converge to a reasonable range. Therefore, the stability and estimated capacity of the observer (19) are verified.

C. SIMULATION OF SET2

To verify tracking performance of the trajectory apart from specific equilibrium point, the desired trajectory of USV in SET2 is selected as (48)-(50) and Fig.6.

$$x_d = \begin{cases} 15\sin(0.2t) & t \leq T_1 \\ 15\sin(0.2(t - T_1)) & T_1 < t \leq T_2 \end{cases} \quad (48)$$

$$y_d = \begin{cases} -15 + 15\cos(0.2t) & t \leq T_1 \\ 15 - 15\cos(0.2(t - T_1)) & T_1 < t \leq T_2 \end{cases} \quad (49)$$

$$\psi_d = \begin{cases} -0.2t & t \leq T_1 \\ 0.2(t - T_1) - 2\pi & T_1 < t \leq T_2 \end{cases} \quad (50)$$

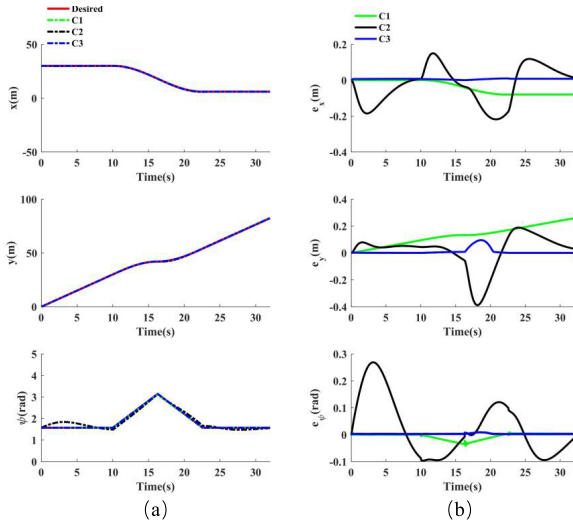


FIGURE 4. The desired trajectory tracking performance of USV in SET1 with C1, C2 and C3.

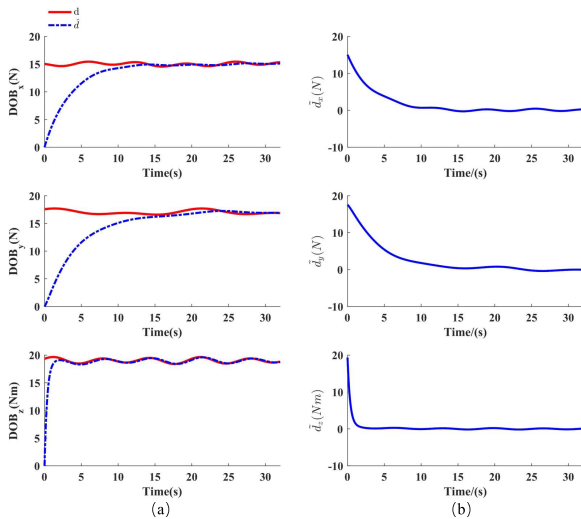


FIGURE 5. The observation performance of observer (19) in SET1.

where $T_1 = 10\pi$, $T_2 = 20\pi$. The initial condition of the USV in SET2 are set as: $x(0) = 0, y(0) = 0, \psi(0) = 0, u(0) = 3, v(0) = 0, r(0) = 0$.

According to the comparative simulation results shown in Fig.7-Fig.8, the USV with different controllers presents good trajectory tracking performance, where the tracking error e and estimate error \tilde{d} are small. Table 3 shows the MIAC value in SET2 with different controllers. It can be

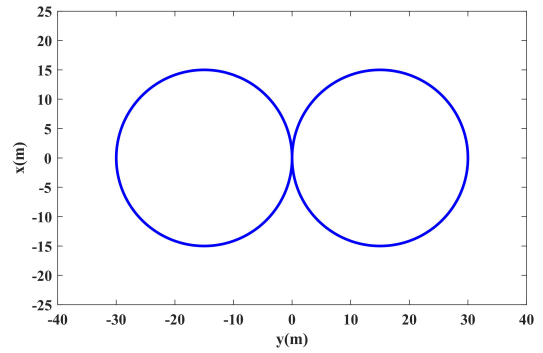


FIGURE 6. The desired trajectory of USV in SET2.

TABLE 3. MIAC of SET2 among different controllers.

MIAC	Value
C1:controller proposed in [11]	$MIAC_{x_e} = 0.0667$
	$MIAC_{y_e} = 0.1301$
	$MIAC_{\psi_e} = 0.0753$
C2:PID controller	$MIAC_{x_e} = 0.0101$
	$MIAC_{y_e} = 0.0111$
	$MIAC_{\psi_e} = 0.0273$
C3:proposed control design	$MIAC_{x_e} = 0.00033$
	$MIAC_{y_e} = 0.0093$
	$MIAC_{\psi_e} = 0.0012$

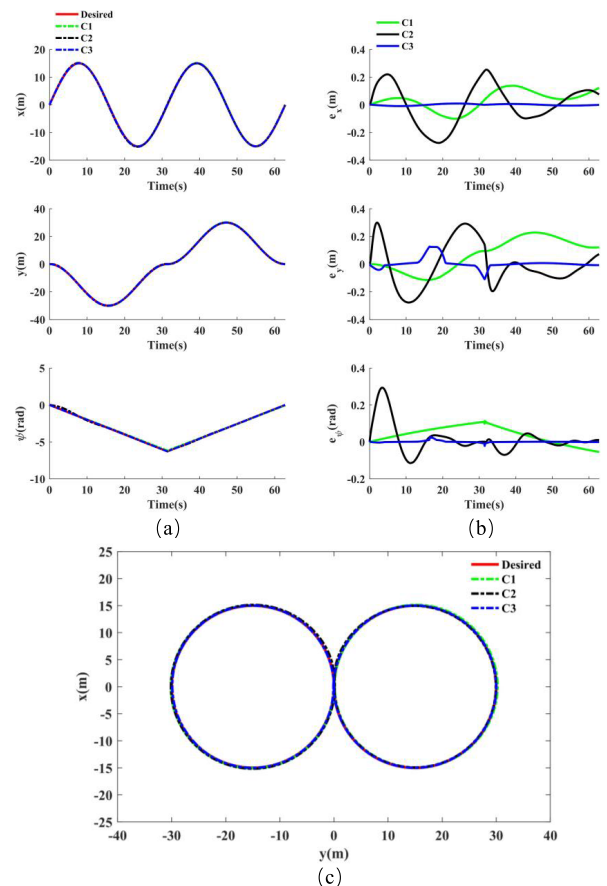


FIGURE 7. The desired trajectory tracking performance of USV in SET2 with C1, C2 and C3.

seen that $MIAC_{x_e}$ of C3 is 0.49% of C1 and 3.27% of C2, $MIAC_{y_e}$ of C3 is 7.15% of C1 and 83.78% of C2, and $MIAC_{\psi_e}$ of C3 is 1.59% of C1 and 4.40% of C2, which

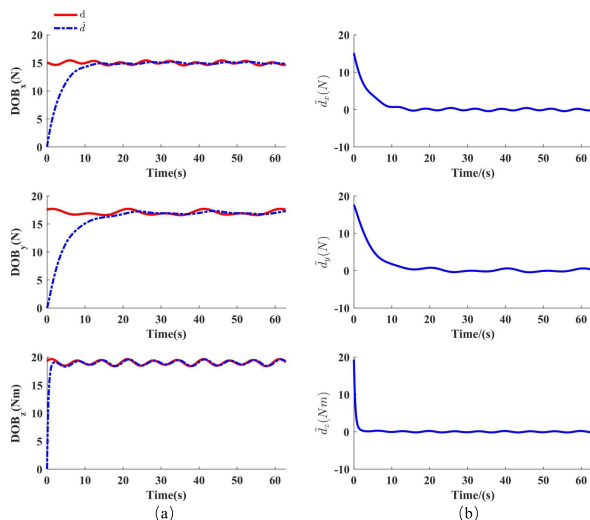


FIGURE 8. The observation performance of observer (19) in SET2.

reflects that the proposed control design has better transient response performance and robustness than linear controller and PID controller with the trajectory apart from the specific equilibrium point.

Based on simulation results with different kinds of trajectory, it can be seen that the proposed control design has the faster response, better transient and robustness compared to linear controller C1 and PID controller C2, which verify the tracking priority and effectiveness of proposed control design.

V. CONCLUSION

In this paper, a disturbance-observer-based sliding mode controller has been proposed for finite-time trajectory tracking of USV based on nonlinear dynamic model with various uncertainties (e.g., modeling error and parameter variations) and external disturbances (wind, wave, current, etc). To estimate the modeling uncertainties and external disturbances, a disturbance observer is designed. Based on the estimated value of observer, a slide-mode controller is developed to track any desired trajectories including straight and other shape, where a saturation function is used to avoid the chattering phenomenon. Moreover, the overall stability of the observer and closed-loop nonlinear system is proved by the Lyapunov stability theorem. Then, a set of comparative trajectory tracking simulation is implemented, where linear controller and PID controller are implemented as comparative object. To evaluate trajectory tracking performance in terms of both transient response and robustness, MIAC index is calculated and results show that the proposed control design has faster response, better transient and robustness compared to other controllers, thus the superiority and effectiveness of proposed controller are verified. In the future, we will consider the impact of control input saturation and violent various external disturbances on system robust stability and tracking performance, and the practical experiments will be considered.

REFERENCES

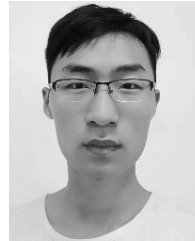
- [1] Z. Dong, L. Wan, Y. Li, T. Liu, and G. Zhang, "Trajectory tracking control of underactuated USV based on modified backstepping approach," *Int. J. Nav. Archit. Ocean Eng.*, vol. 7, no. 5, pp. 817–832, 2015.
- [2] Z. Chen, B. Yao, and Q. Wang, " μ -synthesis-based adaptive robust control of linear motor driven stages with high-frequency dynamics: A case study," *IEEE/ASME Trans. Mechatronics*, vol. 20, no. 3, pp. 1482–1490, Jun. 2015.
- [3] M. Yuan, Z. Chen, B. Yao, and X. Zhu, "Time optimal contouring control of industrial biaxial gantry: A high-efficient analytical solution of trajectory planning," *IEEE/ASME Trans. Mechatronics*, vol. 22, no. 1, pp. 247–257, Feb. 2017.
- [4] Z. Chen, Y.-J. Pan, and J. Gu, "Integrated adaptive robust control for multilateral teleoperation systems under arbitrary time delays," *Int. J. Robust Nonlinear Control*, vol. 26, no. 12, pp. 2708–2728, Aug. 2016.
- [5] X. Sun, G. Wang, Y. Fan, D. Mu, and B. Qiu, "Collision avoidance of podded propulsion unmanned surface vehicle with COLREGs compliance and its modeling and identification," *IEEE Access*, vol. 6, pp. 55473–55491, 2018.
- [6] D. Mu, Y. Zhao, G. Wang, Y. Fan and Y. Bai, "Course control of USV based on fuzzy adaptive guide control," in *Proc. Chin. Control Decis. Conf. (CCDC)*, May 2016, pp. 6433–6437.
- [7] Z. Liu, Y. Zhang, X. Yu, and C. Yuan, "Unmanned surface vehicles: An overview of developments and challenges," *Annu. Rev. Control*, vol. 41, pp. 71–93, Jan. 2016.
- [8] Y. Liu and R. Bucknall, "Efficient multi-task allocation and path planning for unmanned surface vehicle in support of ocean operations," *Neurocomputing*, vol. 275, pp. 1550–1566, Jan. 2018.
- [9] Y.-L. Wang and Q.-L. Han, "Network-based fault detection filter and controller coordinated design for unmanned surface vehicles in network environments," *IEEE Trans. Ind. Informat.*, vol. 12, no. 5, pp. 1753–1765, Oct. 2016.
- [10] D. D. Mu, G. F. Wang, and Y. S. Fan, "Design of adaptive neural tracking controller for pod propulsion unmanned vessel subject to unknown dynamics," *J. Elect. Eng. Technol.*, vol. 12, no. 6, pp. 2365–2377, 2017.
- [11] J. Shin, D. J. Kwak, and Y.-I. Lee, "Adaptive path-following control for an unmanned surface vessel using an identified dynamic model," *IEEE/ASME Trans. Mechatronics*, vol. 22, no. 3, pp. 1143–1153, Jun. 2017.
- [12] N. Wang, Z. Sun, J. Yin, S.-Y. Su, and S. Sharma, "Finite-time observer based guidance and control of underactuated surface vehicles with unknown sideslip angles and disturbances," *IEEE Access*, vol. 6, pp. 14059–14070, 2018.
- [13] N. Wang, Z. Sun, J. Yin, Z. Zou, and S.-F. Su, "Fuzzy unknown observer-based robust adaptive path following control of underactuated surface vehicles subject to multiple unknowns," *Ocean Eng.*, vol. 176, pp. 57–64, Mar. 2019.
- [14] I. S. Edoardo, H. Qu, R. B. Ivan, R. BertaskaKarl, and D. von Ellenrieder, "Station-keeping control of an unmanned surface vehicle exposed to current and wind disturbances," *Ocean Eng.*, vol. 127, no. 1, pp. 305–324, Nov. 2016.
- [15] M. N. Azzeri, F. A. Adnan, and M. M. Zain, "Review of course keeping control system for unmanned surface vehicle," *Jurnal Teknologi*, vol. 74, no. 5, pp. 11–20, 2015.
- [16] T. Liu, Z. Dong, H. Du, L. Song, and Y. Mao, "Path following control of the underactuated USV based on the improved line-of-sight guidance algorithm," *Polish Maritime Res.*, vol. 24, no. 1, pp. 3–11, 2017.
- [17] Y.-L. Liao, M.-J. Zhang, L. Wan, and Y. Li, "Trajectory tracking control for underactuated unmanned surface vehicles with dynamic uncertainties," *J. Central South Univ.*, vol. 23, no. 2, pp. 370–378, 2016.
- [18] A. S. K. Annamalai, R. Sutton, C. Yang, P. Culverhouse, and S. Sharma, "Robust adaptive control of an uninhabited surface vehicle," *J. Intell. Robot. Syst.*, vol. 78, no. 2, pp. 319–338, 2015.
- [19] Y.-L. Wang and Q.-L. Han, "Network-based heading control and rudder oscillation reduction for unmanned surface vehicles," *IEEE Trans. Control Syst. Technol.*, vol. 25, no. 5, pp. 1609–1620, Sep. 2017.
- [20] J. Han, J. Xiong, Y. He, F. Gu, and D. Li, "Nonlinear modeling for a water-jet propulsion USV: An experimental study," *IEEE Trans. Ind. Electron.*, vol. 64, no. 4, pp. 3348–3358, Apr. 2017.
- [21] C. Hu, R. Wang, F. Yan, and N. Chen, "Robust composite nonlinear feedback path-following control for underactuated surface vessels with desired-heading amendment," *IEEE Trans. Ind. Electron.*, vol. 63, no. 10, pp. 6386–6394, Oct. 2016.
- [22] L. P. Perera and C. G. Soares, "Pre-filtered sliding mode control for nonlinear ship steering associated with disturbances," *Ocean Eng.*, vol. 51, pp. 49–62, Sep. 2012.

- [23] B. S. Park, J.-W. Kwon, and H. Kim, "Neural network-based output feedback control for reference tracking of underactuated surface vessels," *Automatica*, vol. 77, pp. 353–359, Mar. 2017.
- [24] B. Qiu, G. Wang, Y. Fan, D. Mu, and X. Sun, "Adaptive sliding mode trajectory tracking control for unmanned surface vehicle with modeling uncertainties and input saturation," *Appl. Sci.*, vol. 9, no. 6, p. 1240, 2019.
- [25] Z. Sun, G. Zhang, L. Qiao, and W. Zhang, "Robust adaptive trajectory tracking control of underactuated surface vessel in fields of marine practice," *J. Mar. Sci. Technol.*, vol. 23, pp. 950–957, Dec. 2018.
- [26] N. Wang, H. R. Karimi, H. Li, and S.-F. Su, "Accurate trajectory tracking of disturbed surface vehicles: A finite-time control approach," *IEEE/ASME Trans. Mechatronics*, vol. 24, no. 3, pp. 1064–1074, Jun. 2019.
- [27] N. Wang, S.-F. Su, X. Pan, X. Yu, and G. Xie, "Yaw-guided trajectory tracking control of an asymmetric underactuated surface vehicle," *IEEE Trans. Ind. Informat.*, vol. 15, no. 6, pp. 3502–3513, Jun. 2019.
- [28] N. Wang, G. Xie, X. Pan, and S.-F. Su, "Full-state regulation control of asymmetric underactuated surface vehicles," *IEEE Trans. Ind. Electron.*, vol. 66, no. 11, pp. 8741–8750, Nov. 2019.
- [29] Z. Chen, B. Yao, and Q. Wang, "Adaptive robust precision motion control of linear motors with integrated compensation of nonlinearities and bearing flexible modes," *IEEE Trans. Ind. Informat.*, vol. 9, no. 2, pp. 965–973, May 2013.
- [30] Z. Chen, C. Li, B. Yao, M. Yuan, and C. Yang, "Integrated coordinated/synchronized contouring control of a dual-linear-motor-driven gantry," *IEEE Trans. Ind. Electron.*, to be published. doi: [10.1109/TIE.2019.2921287](https://doi.org/10.1109/TIE.2019.2921287).
- [31] Z. Chen, F. Huang, C. Yang, and B. Yao, "Adaptive fuzzy backstepping control for stable nonlinear bilateral teleoperation manipulators with enhanced transparency performance," *IEEE Trans. Ind. Electron.*, vol. 67, no. 1, pp. 746–756, Jan. 2020. doi: [10.1109/TIE.2019.2898587](https://doi.org/10.1109/TIE.2019.2898587).
- [32] Z. Chen, F. Huang, W. Chen, J. Zhang, W. Sun, J. Chen, J. Gu, and S. Zhu, "RBFNN-based adaptive sliding mode control design for delayed nonlinear multilateral tele-robotic system with cooperative manipulation," *IEEE Trans. Ind. Informat.*, to be published. doi: [10.1109/TII.2019.2927806](https://doi.org/10.1109/TII.2019.2927806).
- [33] W. Sun, J. Zhang, and Z. Liu, "Two-time-scale redesign for antilock braking systems of ground vehicles," *IEEE Trans. Ind. Electron.*, vol. 66, no. 6, pp. 4577–4586, Jun. 2019.
- [34] W. Sun, Z. Liu, and H. Gao, "Constrained sampled-data ARC for a class of cascaded nonlinear systems with applications to motor-servo systems," *IEEE Trans. Ind. Informat.*, vol. 15, no. 2, pp. 766–776, Feb. 2019.
- [35] J. Yao and W. Deng, "Active disturbance rejection adaptive control of hydraulic servo systems," *IEEE Trans. Ind. Electron.*, vol. 64, no. 10, pp. 8023–8032, Oct. 2017.
- [36] J. Yao, W. Deng, and Z. Jiao, "RISE-based adaptive control of hydraulic systems with asymptotic tracking," *IEEE Trans. Automat. Sci. Eng.*, vol. 14, no. 3, pp. 1524–1531, Jul. 2015.
- [37] Y. Wang, F. Yan, J. Chen, F. Ju, and B. Chen, "A new adaptive time-delay control scheme for cable-driven manipulators," *IEEE Trans. Ind. Informat.*, vol. 15, no. 6, pp. 3469–3481, Jun. 2019. doi: [10.1109/TII.2018.2876605](https://doi.org/10.1109/TII.2018.2876605).
- [38] R. Skjetne, "The maneuvering problem," Ph.D. dissertation, Dept. Eng. Cybern., Norwegian Univ., Sci. Technol., Trondheim, Norway, 2005.
- [39] G. Zhu and J. Du, "Global robust adaptive trajectory tracking control for surface ships under input saturation," *IEEE J. Ocean. Eng.*, to be published. doi: [10.1109/JOE.2018.2877895](https://doi.org/10.1109/JOE.2018.2877895).



YOUGONG ZHANG received the B.Eng. degree in mechanical engineering from Nanchang University, Jiangxi, China, in 2018. He is currently pursuing the M.Eng. degree with the Ocean College, Zhejiang University.

His research interest includes the control of robotics.



YOUMING ZHANG received the B.Eng. degree in measurement and control technology and instrumentation program from the Dalian University of Technology, Dalian, China, in 2018. He is currently pursuing the M.Eng. degree with the Ocean College, Zhejiang University.

His research interest includes the path planning of robotics.



YONG NIE received the Ph.D. degree in mechatronic engineering from Zhejiang University, Zhejiang, China, in 2010, where he is currently a Lecturer with the Mechanical Department.

His research interest includes mechatronics system control and simulator.



JIANZHONG TANG received the Ph.D. degrees in mechatronic control engineering from Zhejiang University, Zhejiang, China, in 2007, where he is currently an Associate Professor in mechanical engineering.

His research interests include robotics and mechatronics.



ZHENG CHEN received the B.Eng. and Ph.D. degrees in mechatronic control engineering from Zhejiang University, Zhejiang, China, in 2007 and 2012, respectively.

From 2013 to 2015, he was a Postdoctoral Researcher with the Department of Mechanical Engineering, Dalhousie University, Halifax, NS, Canada. Since 2015, he has been an Associated Professor with the Ocean College, Zhejiang University. His research interests include advanced

control of robotic and mechatronic systems (e.g., nonlinear adaptive robust control, motion control, trajectory planning, tele-robotics, exoskeleton, mobile manipulator, precision mechatronic systems, and underwater robot).



SHIQIANG ZHU received the B.Eng. degree in mechanical engineering from Zhejiang University, in 1988, the M.Eng. degree in mechatronic engineering from the Beijing Institute of Technology, in 1991, and the Ph.D. degree in mechanical engineering from Zhejiang University, Hangzhou, China, in 1995.

He became a Faculty Member with Zhejiang University, in 1995, and was promoted to the rank of Professor, in 2001, where he is currently with

the Ocean College. His research interests include robotics and mechatronics.

• • •